REKAYASAMESIN V12 N3
eISSN 2477-6041 artikel 9, pp. 591 – 604, 2021

EFFECT OF THE SUBSTRATE SURFACE PROFILE ON THE BONDING STRENGTH OF THE ALUMINUM THERMAL SPRAYED ON THE LOW CARBON STEEL

Nurul Muhayat
Lecturer
Universitas Sebelas Maret
Mechanical Engineering Department

Ilham Habibi
Student
Universitas Sebelas Maret
Mechanical Engineering Department

Teguh Triyono
Lecturer
Universitas Sebelas Maret
Mechanical Engineering Department

Sukmaji Indro Cahyono
Lecturer
Universitas Sebelas Maret
Mechanical Engineering Department

Eko Surojo
Lecturer
Universitas Sebelas Maret
Mechanical Engineering Department

Triyono
Lecturer
Universitas Sebelas Maret
Mechanical Engineering Department
triyono74@staff.uns.ac.id

The contact surface of thermal spray significantly affected bonding strength and coating elasticity. This work aimed to evaluate the effects of contact surface conditions characterised by substrate surface profile and spray pressure on the bonding and buckling strength of aluminium thermal sprayed on the low-carbon steel substrate. The SS400 low-carbon steel substrate was profiled using the milling process to form the V, small V, U, and flat profiles that were subsequently roughed by employing the sandblasting process. A coating comprising 99% aluminium was sprayed onto the substrate surface with different spraying pressures of 3.5, 4.5, and 5.5 bar. Pull-off and buckling tests were performed for determining thermal spray characteristics. The results of this work showed that the optimal bonding strength of the coating was obtained for the thermal spray specimen that had a flat substrate surface, and the spraying pressure was set to 5.5 bar. Generally, low spraying pressure lead to be low bonding strength and vice versa. Profiled surface was not profitable on the mechanic properties of thermal spray bonding.

Keywords: *Aluminum Thermal Sprayed, Surface Profile, Pull-Off, Bonding Strength, Buckling Strength*

1. INTRODUCTION

Surfaces that are subjected to wear and corrosion typically require different characteristics concerning the core and the surface. The coating process is appropriate for determining the best combination of coating and substrate material for a particular application. There are various coating processes such as cladding, chemical vapor deposition, chemical processes, ion implantation, and thermal spraying [1-4]. Thermal spraying has many advantages over other methods. It provides for easy material selection, variants with higher thickness, and good coating properties [1-6]. Figure 1 shows a comparison of the coating processes based on coating thickness and substrate temperature. Thermal spray is one of the coating processes that can be used for metallic or non-metallic substrates [7]. The main group of the thermal spray process consists of several types such as flame spray, electric arc spray, and plasma arc spray.

Electric arc and twin arc spray are types of electric arc spray technique. Twin arc-spray is one of the cheapest thermal spray processes. In this process, the electrodes comprise two wires having the same diameter that lead to simultaneous material spraying. Technology development concerning the arc-spray wire system has promoted numerous applications, such as the mould spray forming [8].

The main properties indicating the quality of the thermal spray process are bonding strength and coating elasticity. The contact surface area between the coating and the substrate affects bond strength. The larger the contact surface, higher is the bonding strength. Coating density and bonding strength affect the coating elasticity. Good coating elasticity is indicated by the absence of coating cracks when the sprayed substrate is bent. Spray material density and bonding strength directly affect coating elasticity [9].

An increase in substrate surface roughness is one way to enhance the contact area between the

Corresponding Author: triyono74@staff.uns.ac.id Received on: March 2021 Accepted on: June 2021
DOI: https://doi.org/10.21776/ub.jrm.2021.012.03.9

substrate and the coating. The expansion of the bonding area increases the bonding strength of the thermal spray coating [9,10]. The expanded contact area also determines bond profiles in the form of the interlocking existing between the substrate and the coating, as shown in Figure 2 [11,12]. There is insufficient information on the relationship between substrate surface profile and bond profile. Previous research has focused on thermal spray and material parameters such as material types, heat treatment, and nozzle spray gun angles. This research, therefore, characterized the tensile strength and buckling strength of the thermally sprayed material using the substrate surface profile and spraying pressures used during thermal spray processes.

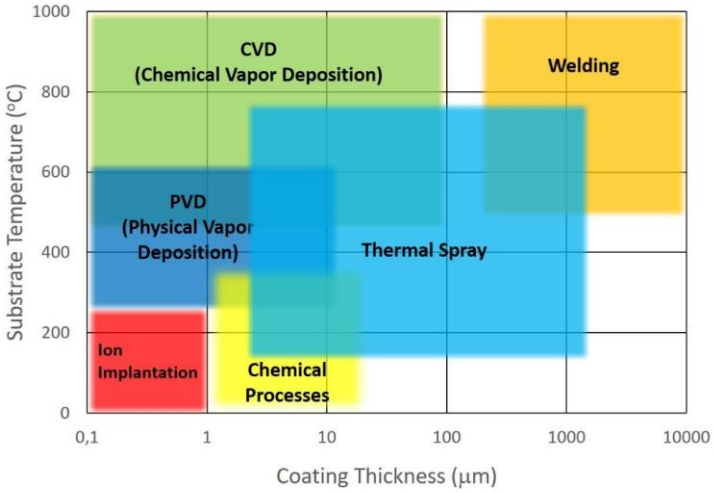

Figure 1. Coating processes comparison [1].

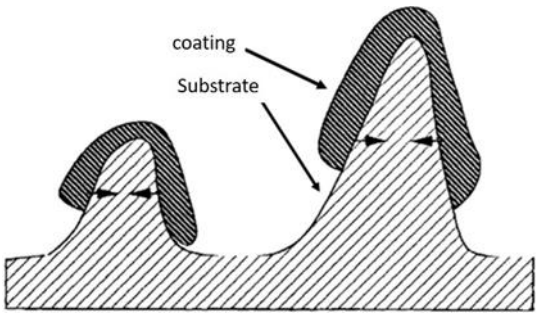

Figure 2. Ilustration of interlocking [2]

2. EXPERIMENTAL METHOD

2.1 Materials and substrate preparation

SS400 low carbon steel substrate was used for experiments. The substrate surface was profiled using the milling process to form a V, small V, and U profile, as shown in Figure 3. The flat surface was also evaluated for comparison. The substrates surfaces were chemically cleaned using Trichloroethylene (TCE) cleaning fluid, rinsed using acetone and then subjected to sandblasting treatment using a steel grid to obtain the constant surface roughness (Ra) of 1.1 □m. The thermal spray uses a twin-arc spray process with AA 1100 aluminium (99% aluminium) wire, 90 ° ± 20° spraying angles with 3.5, 4.5, and 5.5 bar spray pressure values. The coating thickness was kept constant at 0.6 mm for all specimens.

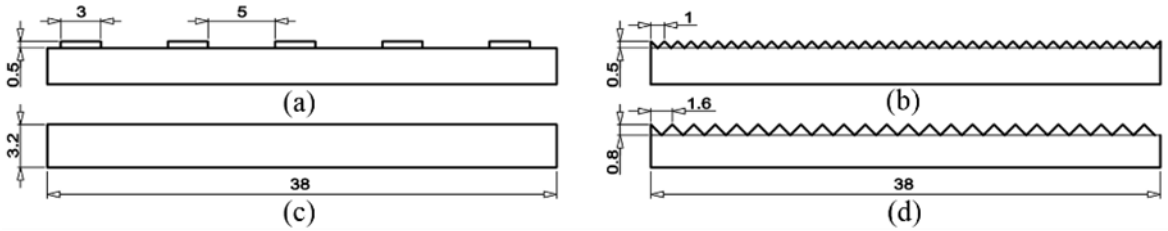

Figure 3. Design of substrate surface profile: (a) U, (b) small V, (c) flat and (d) V

2.2 Coating characterization

The tensile tests for coating were carried out based on the ASTM D4541 standard, which is illustrated in Fig. 4. The buckling tests were adapted using the ASTM E 190 standard, and analysis was performed as suggested by Hafiz et al. [15]. Figure 5 shows the classification of the buckling test results. Microstructure observation aims to determine diffusion and bonding between the coating and the substrate, and it was performed by using a Scanning Electron Microscope (TESCAN Vega3 LMU) with the EDX (OXFORD INCA Energy 250) attached.

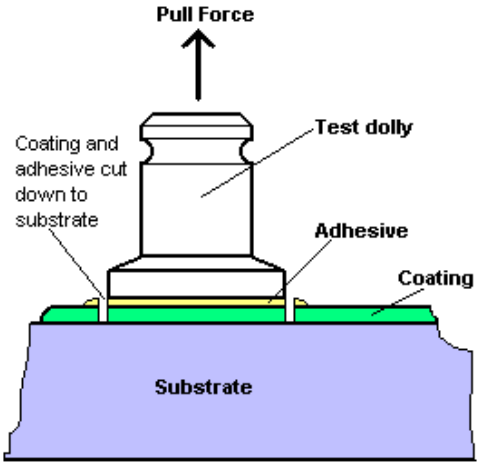

Figure 4. Pull of test scheme [3]

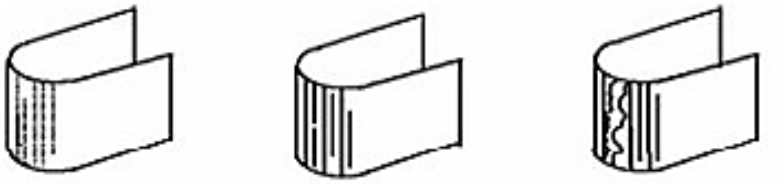

Figure 5. Bend test indicator, (a) no crack, (b) minor cracking, (c) cracks with lifting [3]

3. RESULTS AND DISCUSSION

3.1 Macrostructure of Thermal Sprayed Steel

Figure 6 shows the surface profile of the steel SS400 low carbon after the thermal spraying process. The contour of the thermally sprayed surface follows the profile of the substrate surface except for the small V profile. It is almost similar to a flat surface because the small V profile was shallow and coated by the material entirely, as seen in Figures 6 (a) and 6 (b).

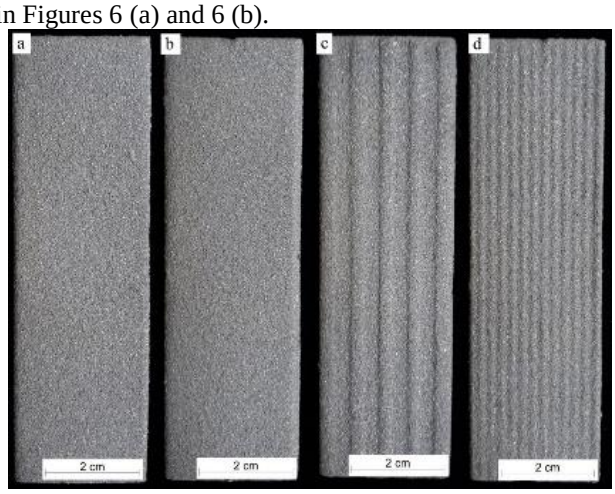

Figure 6. Thermal sprayed steel with (a) flat surface, (b) small V surface, (c) U surface and (d)V surface.

Sandblasting is performed before thermal spraying, where the sandblasted particles hit the surface and

cause erosion at sharp angles, thereby beading to a blunt small V profile. Though the outer surface has an almost similar profile, the interface profile between the coating and the substrate is different for the flat and small V variants. The cross-section of the thermally sprayed substrate is depicted in Figures 7(a) and 7(b). Figure 7 indicates that the interface profile between the coating and the substrate follows the original substrate profile. The V, small V, and U profiles of the substrate surface had wider interface contact compared to the flat substrate profile. The interface contact area between the substrate and coating affects the bonding strength of thermal spray [13].

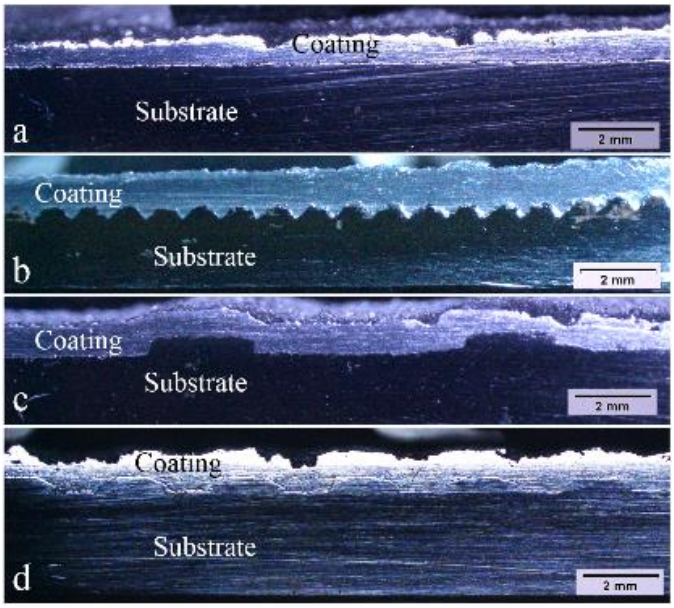

Figure 7. Cross section of thermal sprayed steel with (a) flat surface, (b) small V surface, (c) U surface, (d) V surface.

3.2 Microstructure of Thermal Sprayed Steel

During the thermal spray process, molten material is sprayed onto the substrate surface. Sprayed material forms layers on the surface of the substrate. The morphology of the layers comprises flat and lamellar structures, but there are some defects. Figure 8 depicts the macroscopic image of the interface between the coating and substrate having a V-shaped surface. It shows the presence of cavities and pores. The pores appear on the coating layer and the interface. The pores on the coating layer were created during thermal arc spray process due to the presence of trapped air or gas [14,15]. Pore formation on the coating occurred when the coating material, in the form of semi-liquid droplets, attached and formed a lamellar structure [16,17].

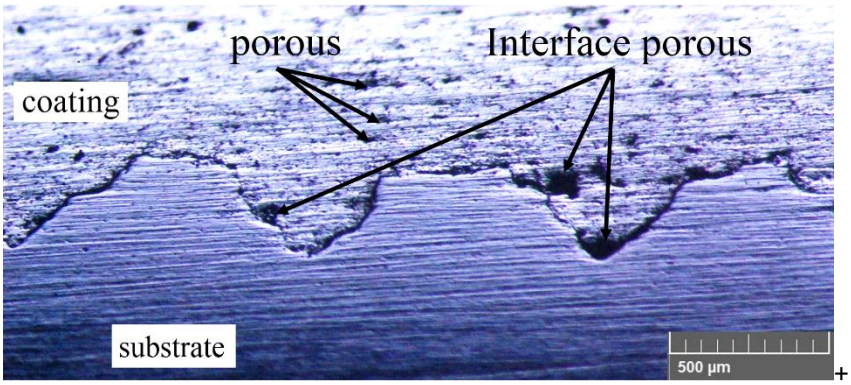

Figure 8. Macrostructure of small V surface profile.

The interface pores depicted in Figure 8 were affected by the substrate surface profile as a result of the sandblasting process conducted before thermal spraying. When sandblasting the V-shaped surface, the sand did not hit the substrate surface perpendicularly, thereby resulting in a rough surface. The mechanism of rough surface formation concerning the V surface during the sandblasting process is depicted in Figure 9. The rough surfaces enable cavities to form on the surface, and the sprayed material does not adhere to the substrate correctly.

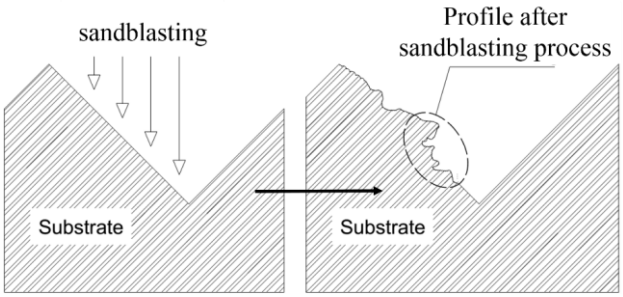

Figure 9. Substrate surface profile (a) before sandblasting process and (b) after sandblasting process.

The thermal spray causes a flat surface profile (Figure 10) which shows that the sprayed material can fill the cavities created by the sandblasting process. The sprayed material made the layers adhere to the substrate surface correctly and also widened the contact surface area. Strong attachment and a wide contact surface lead to an increase in bonding strength [18-23]. In this case, the cavities filled by the sprayed material formed an interlocking structure on the interface between substrate and coating. Interlocking comprises the coating locked on the substrate due to a shrinkage of the layer during the thermal spray process [24-28]. The sandblasted surface had almost uniform cavities, thereby leading to easy interlocking. Higher interlocking between the substrate surface-coating interface leads to higher bonding strength.

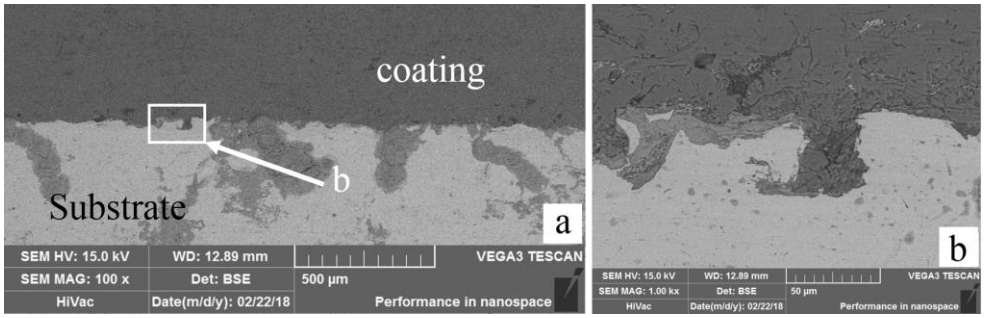

Figure 10. Morphology of the thermal spray layer on the flat surface profile with the spray pressure of 4.5 bar: (a) macro view, (b) detail of b area.

Coating shrinkage also had deleterious effects on bond strength when the substrate surface is flat and lacks cavities. Shrinkage makes stress move away from the substrate. The coating warped and its tip pulled out during shrinkage [29-32]. The scheme of this deleterious shrinkage mechanism was illustrated by Xue et al. [32] and is depicted in Figure 11. Warped coating reduces the contact surface between the coating and substrate and ultimately reduces thermal spray bonding strength.

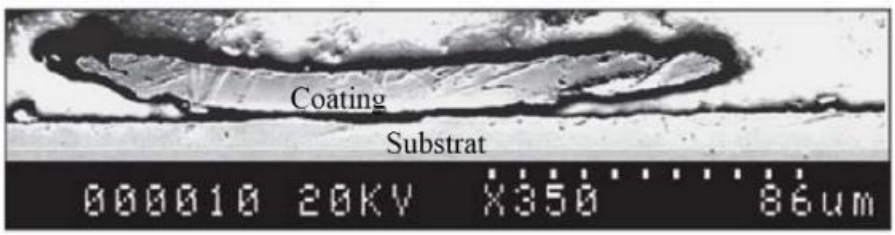

Figure 11. Splats shrinkage [32].

On profiled substrates like V, small V and U surfaces, coating shrinkage had more deleterious effects whereby the shrinkage forces had opposite direction on the peaks and valleys; hence, cracks formed on these parts. Figure 12 illustrates the crack formation mechanism pertaining to the peaks and valleys of the surface profile. Cracked coating reduces contact surface area and the bonding strength of thermally sprayed surface [33-35]. Considering these phenomena, any attempts to expand the contact surface between the coating and substrate by making a profile on the substrate surface were unsuccessful. Flat surface treated using sandblasting appears to be the best method for preparing the substrate surface for the thermal spraying process.

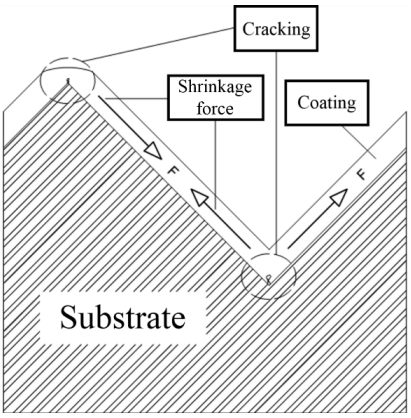

Figure 12. Cracking scheme at the V surface substrate

In this study, in addition to the substrate surface profiles, spray pressure was also evaluated. Based on the overall examination of microstructures, it was determined that spraying pressure had no significant effect on the substrate surface profile. To evaluate the effects of spray pressure on the morphology of the coating-substrate interface, the specimen sprayed at 4.5 bar pressure was considered for experimentation. Figures 13, 14, and 15 show the morphology of coating-substrate interface for small V, V, and U surface profiles, respectively. Two types of defects, namely, cavity and crack, were emphasised to characterise the coating-substrate interface. Small V, V, and U surface profiles had both cavity and cracks on the coating-substrate interface.

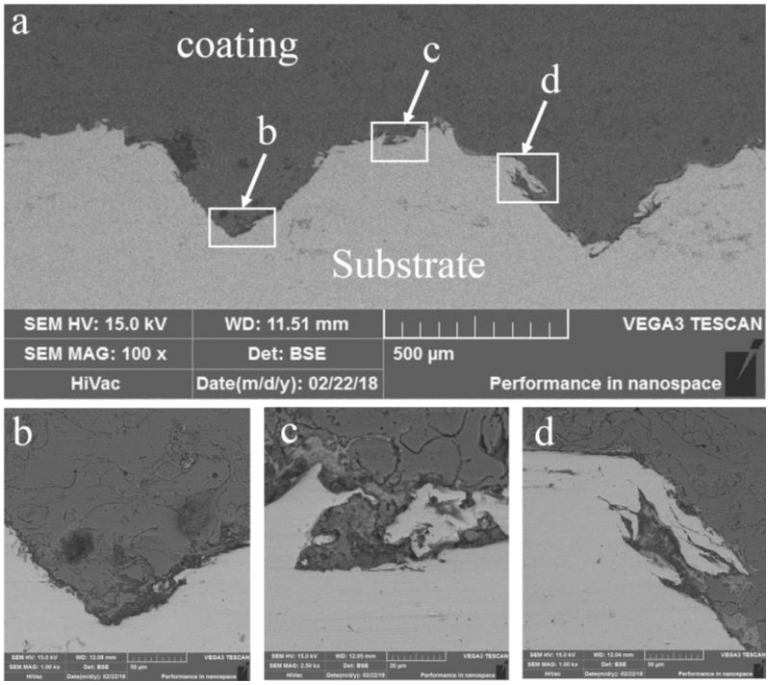

Figure 13. (a) Coating-substrate interface of the small V surface profile with spraying pressure of 4.5 bar, (b) b zone, (c) c zone and (d) d zone.

Figures 13 (c), (d), Figure 14s (a), (c), and Figures 15 (c) (d) show the interface cavity pertaining to the small V, V, and U surface profiles, respectively. Moreover, Figure 13 (b), Figure 14 (b), and Figures 15 (b) and (e) show interface cracking specific to small V, V, and U surface profiles, respectively. These figures confirm the interface cracking and pore formation mechanisms that have been explained and illustrated in Figures 9 and 12.

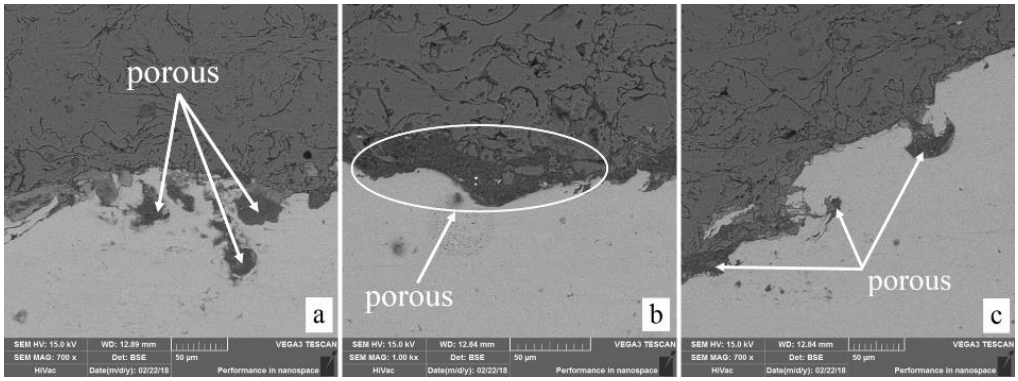

Figure 14. Coating-substrate interface of the V surface profile with spraying pressure of 4.5 bar: (a) hypotenuse zone, (b) valley zone and (c) peak zone.

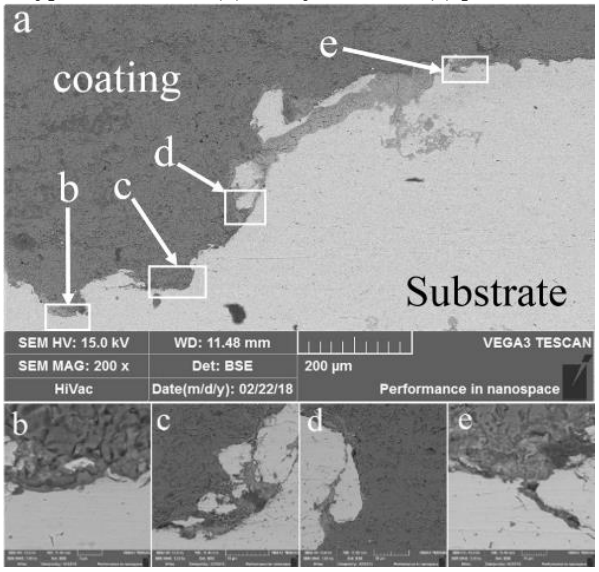

Figure 15. (a) Coating-substrate interface of the U surface profile with spraying pressure of 4.5 bar, (b) b zone, (c) c zone, (d) d zone and (e) e zone.

During the thermal spray process, hot and molten material was sprayed onto the substrate surface. In this study, aluminium was sprayed while the substrate was low carbon steel. Different combinations of heat and pressure were used to spray aluminium onto the substrate and allow the sprayed materials to diffuse into the surface of the substrate material. The diffusion of two or more different elements due to heat and pressure can produce metallurgical bonds [36-39]. Diffusion of elements in the interface between the coating and substrate occurs when the temperature of the sprayed material is sufficient enough to heat the contact surface. The substrate may be in a molten state, and the fusion of two or more elements may occur. It leads to the formation of microscopic alloy on the coating-substrate interface. If the substrate does not melt as a result of the temperature of the sprayed material, high-temperature solid-state diffusion still happens, and a microscopic alloy layer is created [40]. The simultaneous presence of metallurgical and mechanical interlocking bonds on the coating-substrate interface leads to an increase in bonding strength.

This study proved that the surface profile of the substrate had significant effects on the diffusion of materials sprayed onto the substrate surface. Based on EDS results, it was concluded that good diffusion occurred when the sprayed material collides with the substrate surface perpendicularly. Figure 16 illustrates

that the diffusion process on the interface pertinent to the flat surface was adequate. Diffusion occurred on a significant portion of the substrate surface because the hot material sprayed on it collided the substrate perpendicularly. It indicates that the flat substrate surface has the best diffusion. Presence of aluminium (Al) in the substrate material (points 1 and 2) and Iron (Fe) in the coating material (point 3) proved that elemental diffusion occurred during the spraying process.

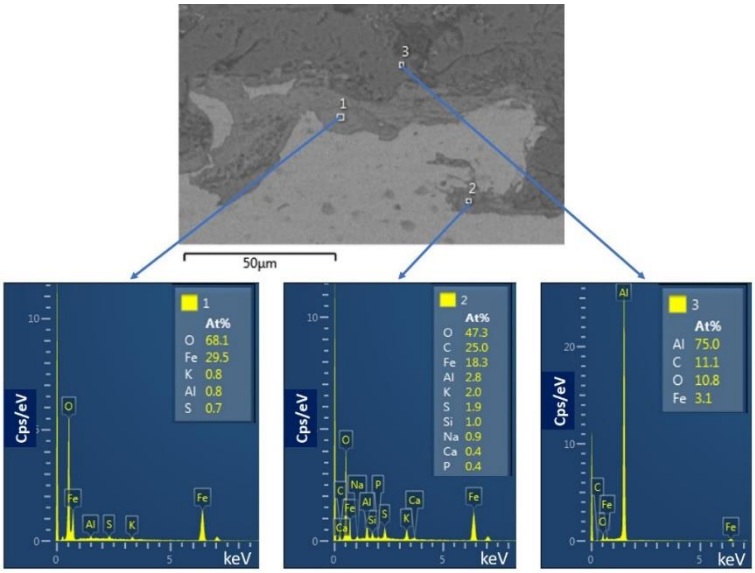

Figure 16. EDS analysis on the coating-substrate interface with a flat profile

Thermal spraying process on the substrate with a small V surface profile made the sprayed material collide with the substrate perpendicularly only on the profile peak (Figure 13c). This area was also observed to have the diffusion of Fe and Al, as depicted in Figure 17. Due to the small pitch between the profile peaks, the small V surface profile had an almost flat surface due to the abrasion on the peak profile as a result of the sandblasting process; this phenomenon is depicted in Figure 7b.

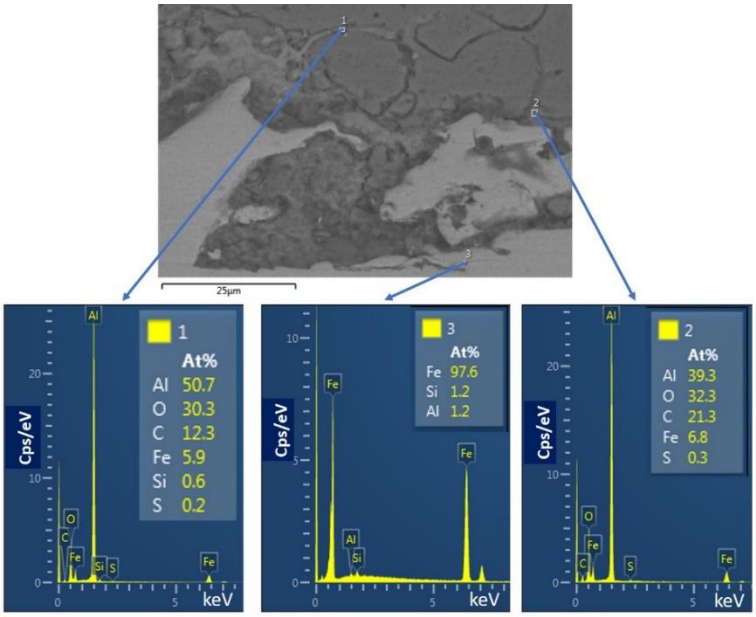

Figure 17. EDS analysis on the coating-substrate interface with small V profile.

The V and U substrate surface profiles had smaller contact surfaces compared to small V and flat

substrate surface profiles. Since diffusion cannot occur in the absence of a contact surface, there was little diffusion of the sprayed material into the substrate on the V and U surface profiles. Figures 18 and 19 depict the small degree of diffusion on the interface between the coating and the substrate pertaining to the V and U surface profiles. Diffusion between two or more elements occurs when there is no cavity or barrier on the coating-substrate interface [41].

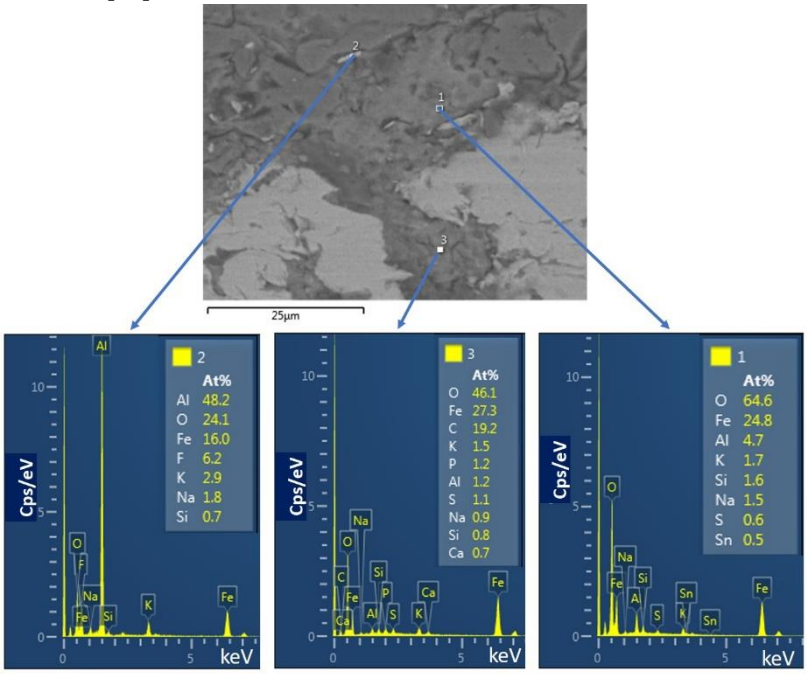

Figure 18. EDS analysis on the coating-substrate interface with U profile.

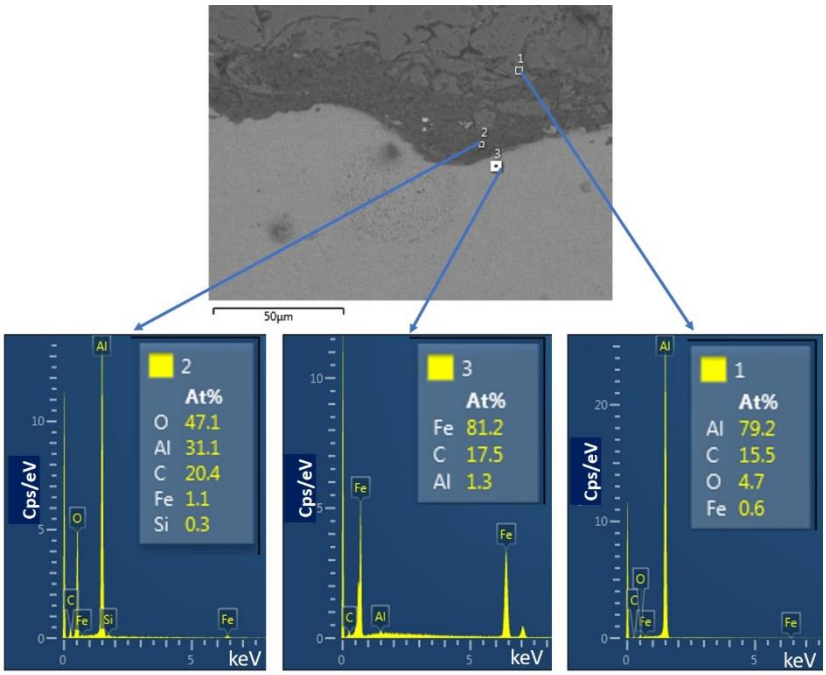

Figure 19. EDS analysis on the coating-substrate interface with V profile.

3.3 Bonding Strength of the Coating

Figure 20 shows that the coating bonding strength when aluminium is sprayed on the low carbon steel substrate is determined by spraying pressure and the surface profile of the substrate. The values for pressure varied and the highest value was 6.24 MPa, while the lowest value was 2.33 MPa. The highest bonding strength was obtained for the specimens having a flat surface profile and spraying pressure of 5.5 bar. In

contrast, the lowest bonding strength was obtained for the specimens having V surface profile and spraying pressure of 3.5 bar. Data fluctuation was notably high but, in general, the pull-off test data were certainly valid since the thermal sprayed coatings got peeled entirely off in a circular manner with a diameter equal to the surface diameter of the pulling device, as depicted in Figure 21. It indicated that the pull-off test results were representative of the real coating bonding strength.

Typically, spraying pressure affects coating bonding strength during the thermal spray process. Higher spraying pressure leads to higher coating bonding strength. Such is the case because of the density of the coating layer sprayed on the substrate. High layer-density is expected to be obtained when there is a significant impact between the sprayed material and the substrate. Impact is driven by spraying pressure. Due to the immense force of the impact, the collisions between sprayed material and substrate surface make the coating flatter and denser.

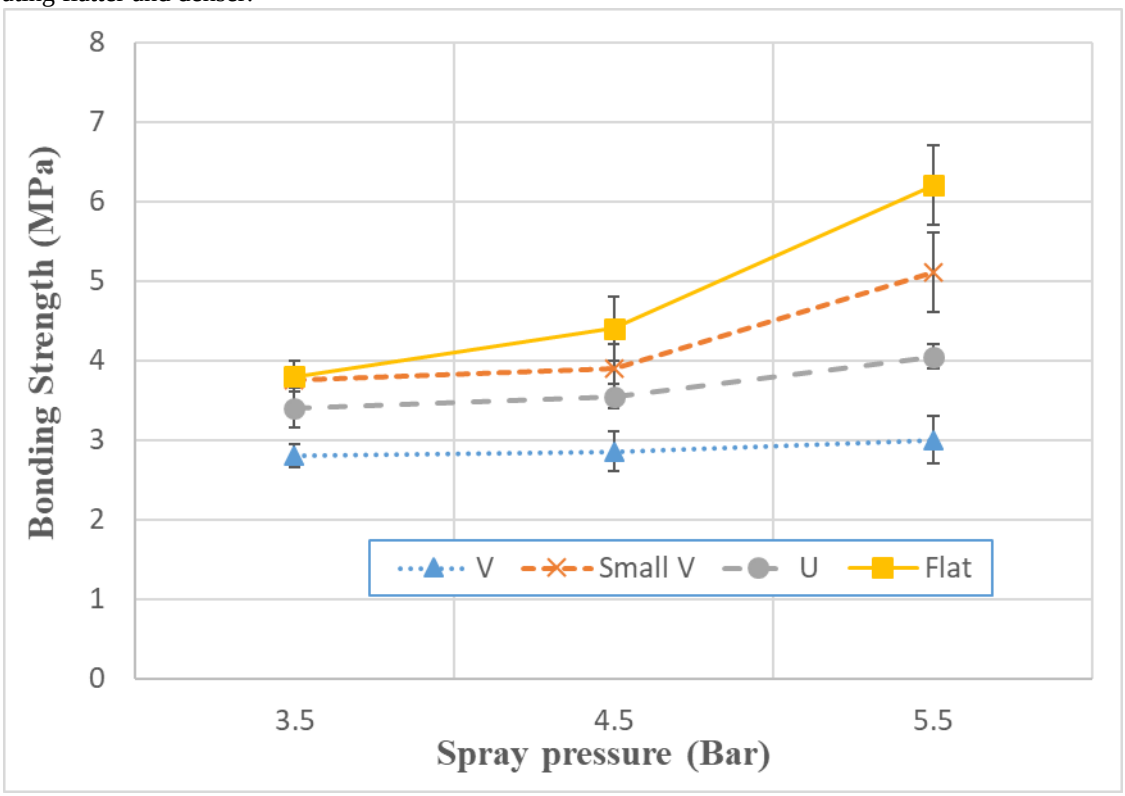

Figure 20. Bonding strength of thermal spray due to spray pressure and substrate surface profile.

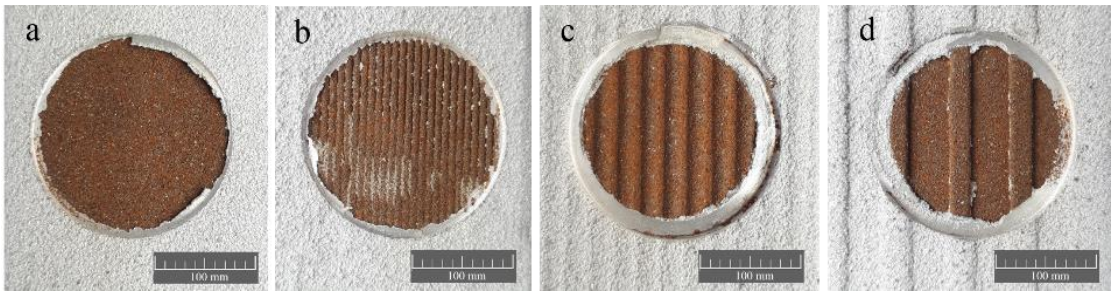

Figure 21. Pull-off testing fracture, (a) flat surface profile, (b) Small V surface, (c) V surface and (d) U surface.

This study proved that the addition of profiles on the substrate surface did not increase the bonding strength specific to thermal spray coating. The profiled surface led to a reduction in the contact surface area between the coating and the substrate as a consequence of surface cavities created due to the non-perpendicular impact during the sandblasting process, as illustrated in Figures 9-15. Surface cavities reduced the contact surface and, therefore, reduced bonding strength [18, 21]. Due to the broader contact surface, the

bonding strength of the thermally sprayed substrate having a flat surface profile was higher compared to other surface profiles irrespective of spraying pressure.

Another factor that affects coating bonding strength is diffusion. Referring to Figures 16-19, it may be observed that a substrate surface having wide flat areas had several sections where diffusion happened. The substrate with a flat surface profile had diffusion across the substrate surface leading to high bonding strength. The small V surface profile had diffusion specific to the profile peak area, as depicted in Figure 13. Due to the small pitch of the peak profile, diffusion specific to the small V surface profile occurred on the wide surface, and its coating bonding strength is very high; however, it remains lower than the coating bonding strength specific to the flat surface specimens. The U and V substrate surface profiles lacked diffusion on hypotenuse parts, as depicted in Figures 14 and 15. Consequently, the coating bonding strength of the U and V substrate surface profile specimens was lower compared to the flat and small V substrate surface profile specimens.

3.4 Buckling Test Results

Buckling test results are divided into three classes: no crack, minor cracks, and cracks with lifting, as illustrated in Figure 5. Coated specimens would meet the no-crack criteria if the buckling force incident on the specimen were not enough to create cracks on the coating. Minor cracking and cracks with lifting criteria are attributed to the coated specimens that not only crack but are also accompanied by the removal of the substrate coating when enough buckling force is incident on the specimens. In the context of this study, all the buckling test specimens were classified as cracks with lifting criteria, as depicted in Figure 22. All coatings lifted and were peeled off the substrate, which indicated that there was low buckling strength pertaining to the thermal sprayed low carbon steel. The strength of the coating material (aluminium) is higher compared to the bonding strength between the coating and the substrate. The tensile strength of aluminium is 80 MPa, while the highest bonding strength observed during this study was merely 6.24 MPa [42].

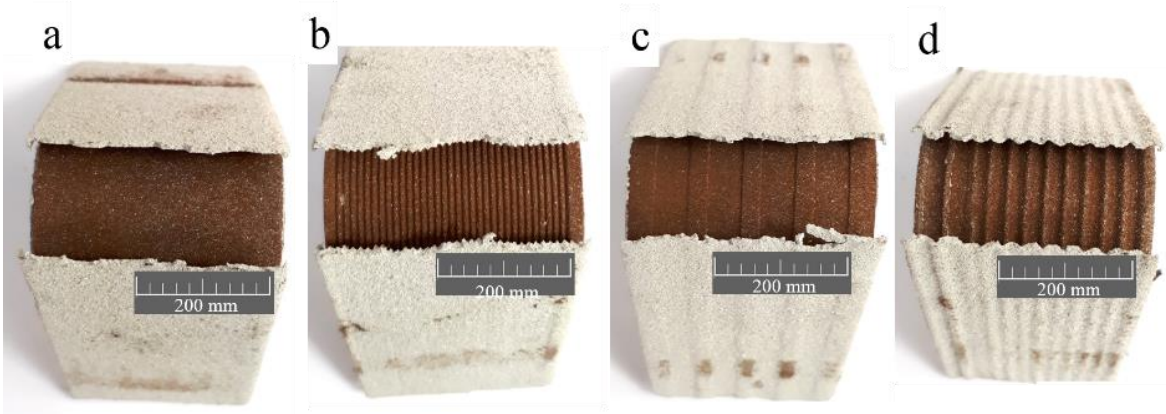

Figure 22. Buckling testing fracture, (a) flat surface profile, (b) Small V surface, (c) U surface and (d) V surface

4. CONCLUSION

The effects of substrate surface profile and spraying pressure on the properties of the aluminium sprayed thermally on low carbon steel were evaluated. The conclusions obtained from this study are as follows:

1. An increase in spraying pressure led to an increase in bonding strength the thermal sprayed coating
2. The flat surface had the best performance due to the simultaneous presence of metallurgical and mechanical interlocking bonds on the substrate-coating interface. The addition of substrate surface profile reduced the bonding strength of the thermal sprayed coating.
3. The profiled surfaces will make high bonding strength of thermal sprayed coating if the sprayed material hit the substrate surface perpendicularly. A special thermal spray gun with a sensor perpendicular to the substrate surface should be designed.
4. The interlocking between the coating and the substrate, cavities on the contact surface, and diffusion on the interface determined bonding strength.

5. ACKNOWLEDGEMENTS

Authors would like to thank a lot to University of Sebelas Maret Surakarta, Indonesia for providing many facilities and financially supporting through Research Group grant with Contract No. **452/UN27.21/PN/2020**.

6. REFERENCES

[1] S. METCO, Material Product Flyer Electric Arc and Combustion Wire Product Portfolio, (2008) 1–4.

[2] S.R. LAMPMAN, W.W. SCOTT, E. MARQUARD, H. LAMPMAN, B. MUSGROVE, K. DRAGOLICH, M. SCHAEFER, ASM Handbook Volume 9 Metallography and Microstructures, ASM Handb. 9 (2004). www.asminternational.org.

[3] F. OTSUBO, H. ERA, AND K. KISHITAKE, Structure and phases in nickel-base self-fluxing alloy coating containing high chromium and boron, *J Therm Spray Tech.*, Vol. 9**,** 107–113 (2000). https://doi.org/10.1361/105996300770350131.

[4] L. LI, X.Y. WANG, G. WEI, A. VAIDYA, H. ZHANG, S. SAMPATH, Substrate melting during thermal spray splat quenching, *Thin Solid Films*, Vol. 468, No. 1-2 (2004) 113–119. doi:10.1016/j.tsf.2004.05.073.

[5] M. BELOTSERKOVSKY, A. YELISTRATOV, A. BYELI, V. KUKAREKO, Steel thermal sprayed coatings: superficial hardening by Nitrogen ion implantation, *Welding Journal*, Vol. 88 (2009).

[6] D.P. CHAKRAVARTHY, D.N. BARVE, D.S. PATIL, P. MISHRA, C.S.R. PRASAD, R.K. ROUT, Development and characterization of single wire-arc-plasma sprayed coatings of nickel on carbon blocks and alumina tube substrates, *Surf. Coatings Technol*. Vol. 202, 325–330 (2007). doi:10.1016/j.surfcoat.2007.05.053.

[7] D. ZOIS, A. LEKATOU, M. VARDAVOULIAS, Preparation and characterization of highly amorphous HVOF stainless steel coatings, *J. Alloys Compd.* Vol. 504 (2010) S283–S287. doi:10.1016/j.jallcom.2010.02.062.

[8] G. JANDIN, H. LIAO, Z.Q. FENG, C. CODDET, Correlations between operating conditions, microstructure and mechanical properties of twin wire arc sprayed steel coatings, *Mater. Sci. Eng. A*. Vol. 349 (2003) 298–305. doi:10.1016/S0921-5093(02)00767-0.

[9] Y. PENG, C. ZHANG, H. ZHOU, L. LIU, On the bonding strength in thermally sprayed Fe-based amorphous coatings, *Surf. Coatings Technol.* Vol. 218 (2013) 17–22. doi:10.1016/j.surfcoat.2012.12.018.

[10] G. J. YANG, C. J. LI, Y. Y. WANG, Phase formation of nano-TiO2 particles during flame spraying with liquid feedstock, *J. Therm. Spray Technol.* Vol. 14 (2005) 480–486. doi:10.1361/105996305X76487.

[11] J. KAWAKITA, T. FUKUSHIMA, S. KURODA, T. KODAMA, Corrosion behaviour of HVOF sprayed SUS316L stainless steel in seawater, *Corros. Sci.* Vol. 44 (2002) 2561–2581. doi:10.1016/S0010-938X(02)00030-6.

[12] M.M. VERDIAN, K. RAEISSI, M. SALEHI, Corrosion performance of HVOF and APS thermally sprayed NiTi intermetallic coatings in 3.5% NaCl solution, *Corros. Sci.* Vol. 52 (2010) 1052–1059. doi:10.1016/j.corsci.2009.11.034.

[13] P. H. GAO, S. T. CAO, J. P. LI, Z. YANG, Y. C. GUO, Y. R. WANG, High temperature oxidation resistance of M42C stainless steel coatings deposited on the surface of cast iron through atmospheric plasma spraying, *J. Alloys Compd.* Vol. 684 (2016) 188–194. doi:10.1016/j.jallcom.2016.05.181.

[14] R. WANG, D. SONG, W. LIU, X. HE, Effect of arc spraying power on the microstructure and mechanical properties of Zn-Al coating deposited onto carbon fiber reinforced epoxy composites, *Appl. Surf. Sci.* Vol. 257 (2010) 203–209. doi:10.1016/j.apsusc.2010.06.065.

[15] M.K. HEDGES, A.P. NEWBERY, P.S. GRANT, Characterisation of electric arc spray formed Ni superalloy IN718, *Mater. Sci. Eng. A.* Vol. 326 (2002) 79–91. doi:10.1016/S0921-5093(01)01431-9.

[16] M.S.A. RAHIM, N. H. SAAD, H.L. BAKIR, Plasma spray ceramic coating and measurement of developed coating behaviour, *International Journal of Precision Technology*, Vol 1 No. 2 (2009) 163–172. doi: 10.1504/IJPTECH.2009.026375

[17] Z. NURISNA, T. TRIYONO, N. MUHAYAT, A.T. WIJAYANTA, Effect of layer thickness on the

properties of nickel Thermal sprayed steel, *AIP Conf. Proc.* 1717 (2016). doi:10.1063/1.4943455.

[18] M.P. KANOUFF, R. A. NEISER JR, T.J. ROEMER, Surface Roughness of *Thermal spray* Coatings Made with Off-Normal Spray Angles, *J. Therm. Spray Technol*. Vol. 7 (1998) 219–228. doi:10.1361/105996398770350963.

[19] L. BAIAMONTE, F. MARRA, S. GAZZOLA, P. GIOVANETTO, C. BARTULI, T. VALENTE, G. PULCI, Surface and coatings technology thermal sprayed coatings for hot corrosion protection of exhaust valves in naval diesel engines, *Surf. Coat. Technol*. Vol. 295 (2016) 78–87. doi:10.1016/j.surfcoat.2015.10.072.

[20] S. COSTIL, H. LIAO, O. CHRETIEN, A. LOREDO, A. GAMMOUDI, M. VERDIER, C. CODDET, Influence of laser surface cleaning combined with substrate laser preheating on Thermal spray coating adhesion, *Lasers Eng.* Vol. 15 (2005) 325–345.

[21] S. DANOUNI, A. ABDELLAH EL-HADJ, M. ZIRARI, M. BELHARIZI, A thermo-mechanical analysis of a particle impact during thermal spraying, *Appl. Surf. Sci.* Vol. 371 (2016) 213–223. doi:10.1016/j.apsusc.2016.02.226.

[22] C. ZHANG, H. ZHOU, L. LIU, Laminar Fe-based amorphous composite coatings with enhanced bonding strength and impact resistance, *Acta Mater.* Vol. 72 (2014) 239–251. doi:10.1016/j.actamat.2014.03.047.

[23] A. EDRISY, T. PERRY, Y. CHENG, A. ALPAS, Wear of thermal spray deposited low carbon steel coatings on aluminum alloys, *Wear* Vol. 251 (2001) 1023–1033. doi:10.1016/S0043-1648(01)00718-9.

[24] Y. C. YANG, E. CHANG, Influence of residual stress on bonding strength and fracture of plasma-sprayed hydroxyapatite coatings on Ti-6Al-4V substrate, *Biomaterials* Vol. 22 (2001) 1827–1836. doi:10.1016/S0142-9612(00)00364-1.

[25] A.S.M. ANG, N. SANPO, M.L. SESSO, S.Y. KIM, C.C. BERNDT, Thermal spray maps: Material genomics of processing technologies, *J. Therm. Spray Technol.* Vol. 22 (2013) 1170–1183. doi:10.1007/s11666-013-9970-3.

[26] K.T. OH, Y.S. PARK, Plasma-sprayed coating of hydroxylapatite on super austenitic stainless steels, *Surf. Coatings Technol.* Vol. 110 (1998) 4–12. doi:10.1016/S0257-8972(98)00537-4.

[27] M.A. MULERO, J. ZAPATA, R. VILAR, V. MARTÍNEZ, R. GADOW, Automated image inspection system to quantify thermal spray splat morphology, *Surf. Coatings Technol*. Vol. 278 (2015) 1–11. doi:10.1016/j.surfcoat.2015.07.065.

[28] L. PAWLOWSKI, The Science and engineering of thermal spray coatings, Wiley; 2nd edition, 2008. doi:10.1002/9780470754085.

[29] S. SAMPATH, J. MATEJICEK, Intrinsic residual stresses in single *splats* produced by thermal spray, *Acta Mater*. Vol. 49 (2001).

[30] R.S.C. PAREDES, S.C. AMICO, A.S.C.M. D'OLIVEIRA, The effect of roughness and pre-heating of the substrate on the morphology of aluminium coatings deposited by Thermal spraying, *Surf. Coatings Technol*. Vol. 200 (2006) 3049–3055. doi:10.1016/j.surfcoat.2005.02.200.

[31] V. V SOBOLEV, J.M. GUILEMANY, The formation of coating shrinkage porosity in the process of thermal spraying, *J. Mater. Process. Technol.* Vol. 58 (1996).

[32] M. XUE, S. CHANDRA, J. MOSTAGHIMI, Investigation of splat curling up in thermal spray coatings, *J. Therm. Spray Technol.* Vol. 15 (2006). doi:10.1361/105996306X147315.

[33] N. NAYEBPASHAEE, S.H. SEYEDEIN, M.R. ABOUTALEBI, H. SARPOOLAKY, S.M.M. HADAVI, Finite element simulation of residual stress and failure mechanism in plasma sprayed thermal barrier coatings using actual microstructure as the representative volume, *Surf. Coatings Technol.* Vol. 291 (2016) 103–114. doi:10.1016/j.surfcoat.2016.02.028.

[34] R.T.R. MCGRANN, D.J. GREVING, J.R. SHADLEY, E.F. RYBICKI, T.L. KRUECKE, B.E. BODGER, The effect of coating residual stress on the fatigue life of thermal spray-coated steel and aluminum, *Surf. Coatings Technol.* Vol. 108–109 (1998) 59–64. doi:10.1016/S0257-8972(98)00665-3.

[35] T.W. CLYNE, S.C. GILL, Residual Stresses in thermal spray coatings and their effect on interfacial adhesion: a review of recent work, *J. Therm. Spray Technol*. Vol. 5 (1996) 401. doi:10.1007/BF02645271.

[36] C. ZHANG, H. LI, M.Q. LI, Detailed analysis of surface asperity deformation mechanism in diffusion bonding of steel hollow structural components, *Appl. Surf. Sci.* Vol. 371 (2016) 407–414. doi:10.1016/j.apsusc.2016.03.039.

[37] H. LI, C. ZHANG, H. BIN LIU, M.Q. LI, Bonding interface characteristic and shear strength of diffusion bonded Ti-17 titanium alloy, *Trans. Nonferrous Met. Soc. China* (English Ed.) Vol. 25 (2015) 80–87. doi:10.1016/S1003-6326(15)63581-6.

[38] B. WANG, F. ZHANG, S.L. CHEN, S. KOU, Computational simulation of diffusion process in multicomponent and multiphase systems in diffusion bonding, *Sci. Technol. Weld. Join.* Vol. 18 (2013) 451–457. doi:10.1179/1362171813Y.0000000121.

[39] L. ZHUANG, Y. LEI, S. CHEN, L. HU, Q. MENG, Microstructure and mechanical properties of AlMgB14-TiB2associated with metals prepared by the field-assisted diffusion bonding sintering process, *Appl. Surf. Sci.* Vol. 328 (2015) 125–132. doi:10.1016/j.apsusc.2014.11.127.

[40] ASM International®, Handbook of Thermal Spray Technology, Materials Park, USA, 2004.

[41] B. WIELAGE, H. POKHMURSKA, M. STUDENT, V. GVOZDECKII, T. STUPNYCKYJ, V. POKHMURSKII, Iron-based coatings arc-sprayed with cored wires for applications at elevated temperatures, *Surf. Coatings Technol.* Vol. 220 (2013) 27–35. doi:10.1016/j.surfcoat.2012.12.013.

[42] ASM Handbook, Volume 2B: Properties and Selection of Aluminum Alloys, ASM Digital Library.